

Estimating Winds from Synthetic Aperture Radar under Typhoon Conditions

Jochen Horstmann

Center for Maritime Research and Experimentation,
Viale San Bartolomeo 400, 19126 La Spezia, Italy

phone: (+39) 0187-527 381 fax: (+39) 0187-527 354 email: Horstmann@cmre.nato.int

Award Number: N0001412WX20895

<http://www.eol.ucar.edu/projects/itop/>

LONG-TERM GOALS

The Impacts of Typhoons on the Ocean in the Pacific (ITOP) program is a multi-national field campaign that aims to study the ocean response to typhoons in the western Pacific Ocean. The main goals are to understand the formation and dissipation of cold wakes and how ocean eddies affect typhoons. CMRE's activities within ITOP are related to SAR wind retrieval and therefore will be helping to better understand air-sea fluxes under extreme wind speeds and improve the knowledge and forecast of surface wave field under typhoons as well as the Typhoon forecasting.

OBJECTIVES

CMRE (former NATO Undersea Research Center) is part of the ITOP SAR Team working on extracting wind and wave information from synthetic aperture radar (SAR) data. Their major objectives are the development and implementation of a SAR Typhoon Processing System (SARTyPS) for near real time processing of SAR data with respect to estimating wind and sea state under tropical cyclone conditions. It is anticipated to incorporate the SAR-retrieved information into numerical models in particular with respect to tropical cyclone forecasting.

The main objectives for CMRE are the development of algorithms that are capable of extracting wind information from SAR images in near real time and fully automated. The SAR activity within ITOP is a close cooperation with the Center for Southeastern Tropical Advanced Remote Sensing (CSTARS) of the University of Miami, General Dynamics Advanced Information Systems (GDAIS) and the Applied Physics Laboratory (APL) of the University of Washington.

APPROACH

In a first step prior to wind retrieval all SAR data have to be accurately calibrated for the normalized radar cross section (NRCS). In addition all acquisitions performed in the scanning mode also have to be corrected for scalloping (Romeiser et al., 2012) as well as beams and nadir ambiguities. SAR data, which were acquired at cross polarization (pol) have to be corrected for the contribution of the noise-equivalent sigma naught (noise floor) of the system to the NRCS. Following these data calibration steps the wind retrieval can be undertaken. In case of SAR data collected at C- and X-band in co-pol, meaning vertical (V) or horizontal (H) polarization in transmit and receive, the detailed methodology

was reported in CMRE's ONR report 2011 (Horstmann, 2011). Wind directions are extracted from wind-induced phenomena that are aligned in wind direction. Within this process pixels associated to land, surface slicks, and strong rain, are masked and excluded from the analysis (Horstmann et al., 2002; Horstmann and Koch, 2005). To reduce the probability of outliers in the wind direction retrieval, CMRE's wind directions were merged with the results obtained from the projection method developed by GDAIS (Wackerman et al., 2003). Wind speeds are retrieved utilizing a geophysical model function (GMF) that describes the dependency of the NRCS on the local near-surface wind and imaging geometry. For C-band VV-pol we utilize the most commonly used GMF CMOD5n (Hersbach, 2010) and in case of HH-pol a hybrid model function which consists of a C-band polarization ratio (PR) and the CMOD5n (Horstmann et al., 2002). For retrieval of wind speeds from SAR operating at X-band, CMRE has developed an empirical GMF for both VV and HH polarization (Thompson et al., 2012). In addition to the high-resolution wind fields we have developed a scheme to estimate the certainty of the retrieved wind speed at every SAR retrieved data point. Furthermore, we generate a mask identifying the regions that give NRCS's that are close or out of the definition range of the utilized GMF. These limitations for co-pol imagery depend on wind direction and incidence angle and only occur at incidence angles below 35° , in particular near to up- and down-wind direction with respect to the radar look (also reported in Horstmann, 2011).

In case of cross pol data (HV or VH pol) the backscatter of the ocean is so low, that to, date only Radarsat-2 data can be utilized for wind retrieval. The noise floor level and/or cross talk (Touzi et al., 2010) of all other space borne SARs is too high, giving NRCS values useless with respect to SAR wind speed retrieval. In case of Radarsat-2 imagery, to get an accurate estimate of the cross pol NRCS, the data have to be corrected for the contribution of the noise floor to the measured NRCS. We have developed a GMF for noise floor corrected Radarsat-2 ScanSAR data acquired at HV pol and VH pol, which describes the dependencies of the NRCS on the wind speed and wind direction (Horstmann et al., 2012).

WORK COMPLETED

In 2012 we have further developed and improved the software package which corrects the SAR data prior to the wind retrieval. Within this process the SAR data are corrected for radiometric calibration, scalloping (Romeiser et al., 2012) as well as beams and nadir ambiguity lines. In case of Radarsat-2 cross pol data the contribution of the noise floor to the NRCS is removed in addition (Horstmann et al., 2012). The noise floor removal schemes for co-pol data of all the available SAR satellites (Envisat, Rsat-1 and -2, TerraSAR-X and Cosmo SkyMed) are being implemented and will be investigated. However, the impact on the wind retrieval at co-pol is expected to be negligible. Figure 1 depicts the different correction steps for a Rsat-2 ScanSAR image, which was acquired at cross-pol (HV pol) on the 22 September 2010, during the ITOP experiment. Cross pol data are due to the very low backscatter from the ocean, which is very close and sometimes even below the noise floor level (in case of Rsat-2 ScanSAR's at $-28 \text{ dB} \pm 2 \text{ dB}$). Therefore, it is essential to remove the contribution of the noise floor to the NRCS prior to wind retrieval. As can be seen in Figure 2, the noise floor varies strongly in range and therefore would add to wind variation if not removed for. Figure 2 also shows the change of the NRCS over range due to the different correction steps applied. It is particularly important to correct for the noise floor when the measured NRCS gets close to the noise floor (near range in Figure 2).

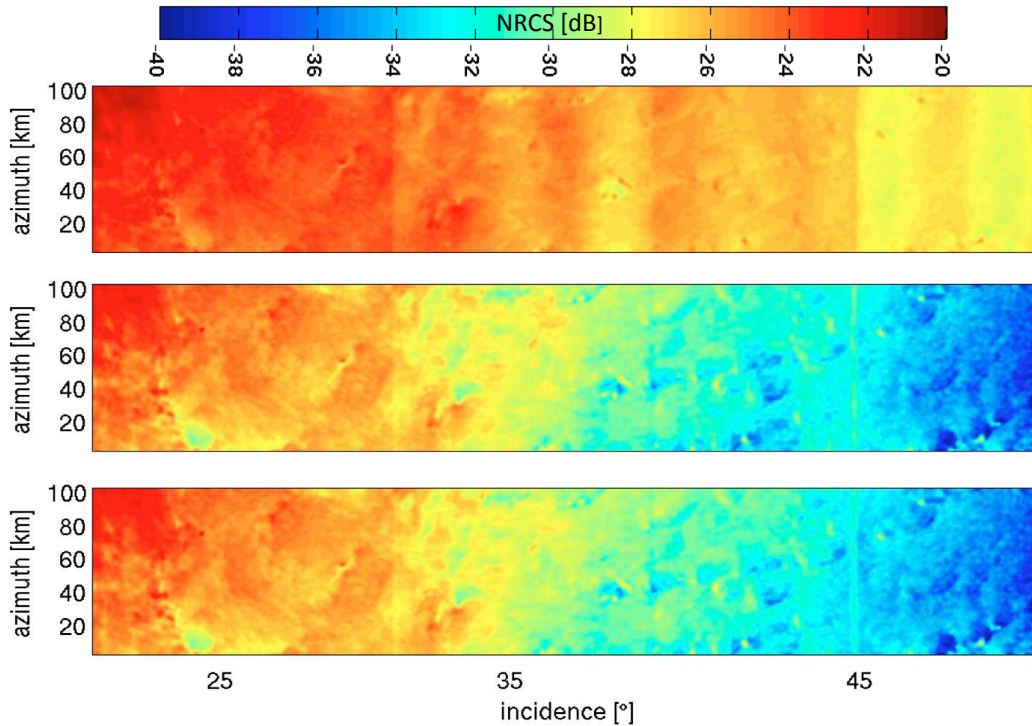


Figure 1: Subimage of the Radarsat-2 ScanSAR image acquired at C-band in cross polarization (*pol*) on the 22 September 2010 at 20:30 UTC depicting the different correction steps applied to the data. Depicted are from top to bottom the original image, image corrected for scalloping and noise floor, and image corrected for the beams and nadir ambiguity lines.

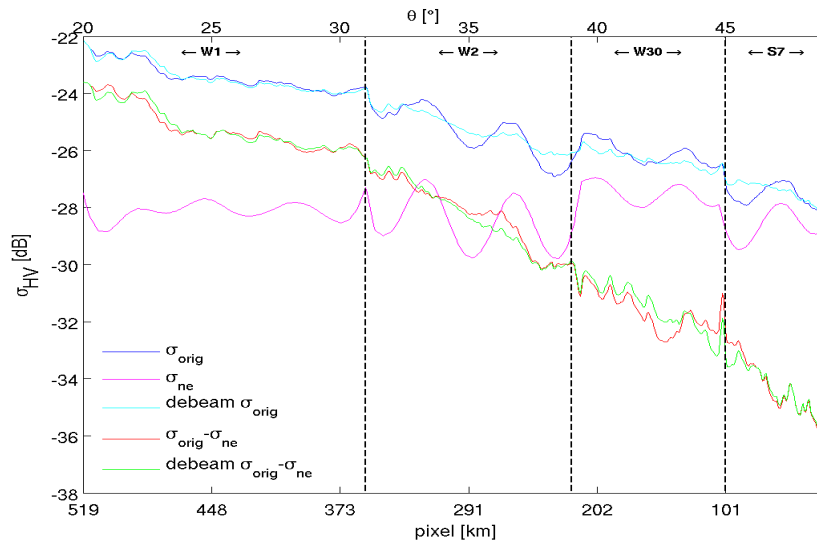


Figure 2: The mean normalized radar cross section (NRCS) over a 100 km azimuth is plotted for the different correction steps applied to the sub-image shown in Figure 1. The vertical dashed lines mark the different beams, which are utilized to generate the ScanSAR image. The blue and cyan curves are the original NRCS and its correspondent beams removed NRCS, respectively. The magenta curve shows the noise equivalent sigma naught values along range. The red and green curves are original NRCS with noise floor removed and the correspondent beams removed product, respectively.

In 2011 we had tested and validated the wind retrieval schemes for C-band co-pol data under consideration of co-located QuikSCAT data. The resulting root mean square (rms) error was 17.6° with a bias of 6.4° showing too much inflow in the SAR retrieved winds. The rms error for wind speeds was 4.6 m/s with a bias of -1.3 m/s (Horstmann, 2011). However, the comparison was mainly considering moderate wind speeds and there were very few QuikSCAT data points available at wind speeds above 25 m/s. During the ITOP experiment in 2010 several SAR data have been collected at CSTARS utilizing SARs operating at C- and X-band with different polarizations (details are given in Tab.1). We have converted all the SAR data to wind fields and compared the C-band co-pol retrieved wind fields to wind speed measurements obtained by SFMR and Dropsonde (Tab. 1). Prior to comparison with SAR winds, the flight tracks were adjusted to the SAR image acquisition time by using the Hurricane Research Division Willoughby center fixes. The scatter plot of the comparison is depicted in Figure 5 (left hand side) resulting in a standard deviation of 5.9 m/s and a bias of 0.38 m/s, with a significant increase of error with increasing speeds.

Table 1: Overview of SAR data acquired during the ITOP experiment. Hurricane Earl was not acquired within the ITOP experiments, but considered within our developments with respect to cross pol data. The red and blue dot indicate the data utilized for our co-pol and cross pol wind speed comparison to SFMR and Dropsonde.

Storm	Acquisition Date mm/dd/yyyy hh:mm	Satellite	Polarization	Saffir-Simpson Hurricane scale	Available Measurements
Earl	09/02/2010 22:59	RS2	VV/VH	2	SFMR; Dropsonde
• Fanapi	09/12/2010 20:23	RS2	VV	Tropical Depression	SFMR; Dropsonde
Fanapi	09/13/2010 09:08	RS2	HH/HV	Tropical Depression	
•• Fanapi	09/17/2010 21:14	RS2	HH/HV	2	SFMR; Dropsonde
•• Malakas	09/22/2010 20:29	RS2	HH/HV	Tropical Storm	SFMR; Dropsonde
Malakas	09/24/2010 08:49	RS2	HH/HV	2	
Malakas	09/29/2010 08:27	CSK-3	VV	(Cold Wake)	
Megi	10/14/2010 09:03	RS2	HH/HV	Tropical Storm	
Megi	10/14/2010 20:58	CSK-3	VV	1	SFMR; Dropsonde
Megi	10/14/2010 21:17	CSK-2	VV	2	SFMR; Dropsonde
Megi	10/15/2010 21:00	RS2	VV	2	SFMR; Dropsonde
Megi	10/16/2010 09:17	CSK-3	VV	3	
• Megi	10/17/2010 01:27	ENVI	VV	5	SFMR; Dropsonde
Megi	10/17/2010 09:35	CSK-3	VV	5	SFMR; Dropsonde
Megi	10/17/2010 21:41	RS2	VV	5	
Megi	10/17/2010 21:53	CSK-3	VV	5	
Megi	10/18/2010 22:12	CSK-3	VV	2	
Megi	10/19/2010 09:41	CSK-1	VV	3	
Megi	10/19/2010 22:30	CSK-3	VV	4	
Megi	10/21/2010 22:05	TSX	VV	2	

To develop a cross pol GMF we investigated the dependencies of the NRCS on wind speed and wind direction utilizing the co-pol retrieved winds as well as the SFMR wind speeds. In Figure 3 the dependency of the cross pol NRCS on wind speed is shown for NRCS that were corrected for the noise floor, scalloping, beams and nadir ambiguity lines. The wind speeds corresponding to the density plot correspond to the Radarsat-2 co-pol retrieved winds. In addition we plotted all the additional available

wind speed data listed in the legend (SFMR, Dropsonde, ASCAT and Windsat). Both the SAR retrieved wind speeds and other available wind speeds show a non linear dependence of the NRCS on wind speed as well as an increasing spread with decreasing wind speeds. Of course the noise floor correction have a greater effect on the lower backscatter values, and for values near to the noise floor the uncertainty of the noise floor will add to inaccuracies of the NRCS. In addition we investigated the dependence of the NRCS on incidence angle and wind direction. In general the incidence angle dependence is small and can be neglected. However, for wind directions a clear dependence was observed in particular at lower wind speeds. The color coded curves show our fitted empirical GMF for different wind directions (up-down wind, cross wind as well as 45° shifted to cross wind). For retrieving the wind speeds from cross pol data we utilize the wind directions retrieved from the co-pol data together with the cross pol NRCS. For high wind (greater than 23m/s) the wind direction dependency is negligible and the suggested GMF shows a linear trend found by only fitting to SFMR ground truth data. The red dashed line represents a GMF, which is independent of wind direction.

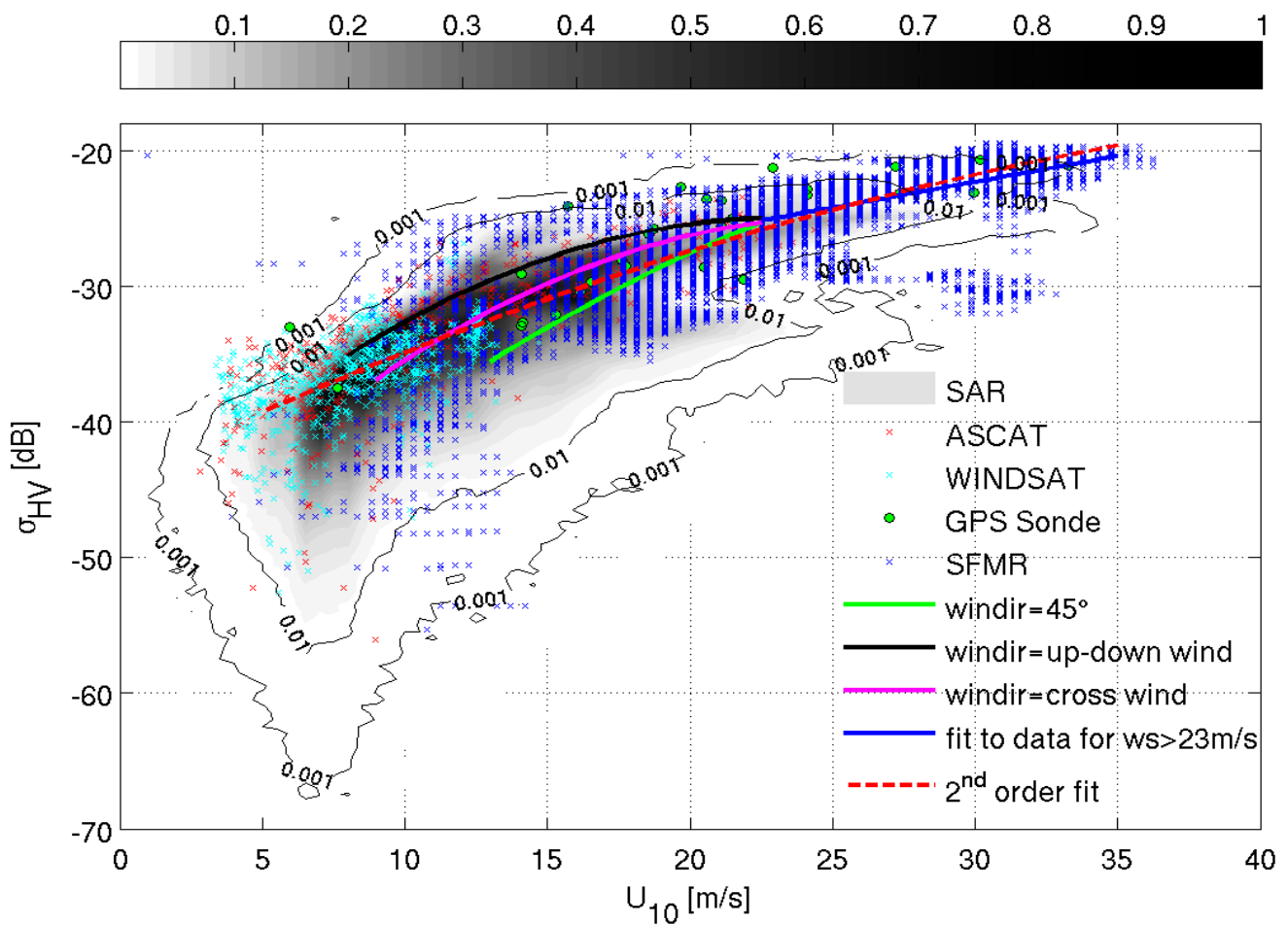


Figure 3: Dependency of cross pol NRCS on wind speed considering all Radarsat-2 ScanSAR scenes listed in Table 1. The underlying density plot and contour lines represent the co-pol retrieved wind speed versus cross pol NRCS. The superimposed color-coded symbols represent the different available wind speed measurements and the corresponding cross pol NRCS. Superimposed red dashed line is the best fit considering no wind direction dependence. The solid lines give the best fits under consideration of the wind direction with respect to the antenna look direction.

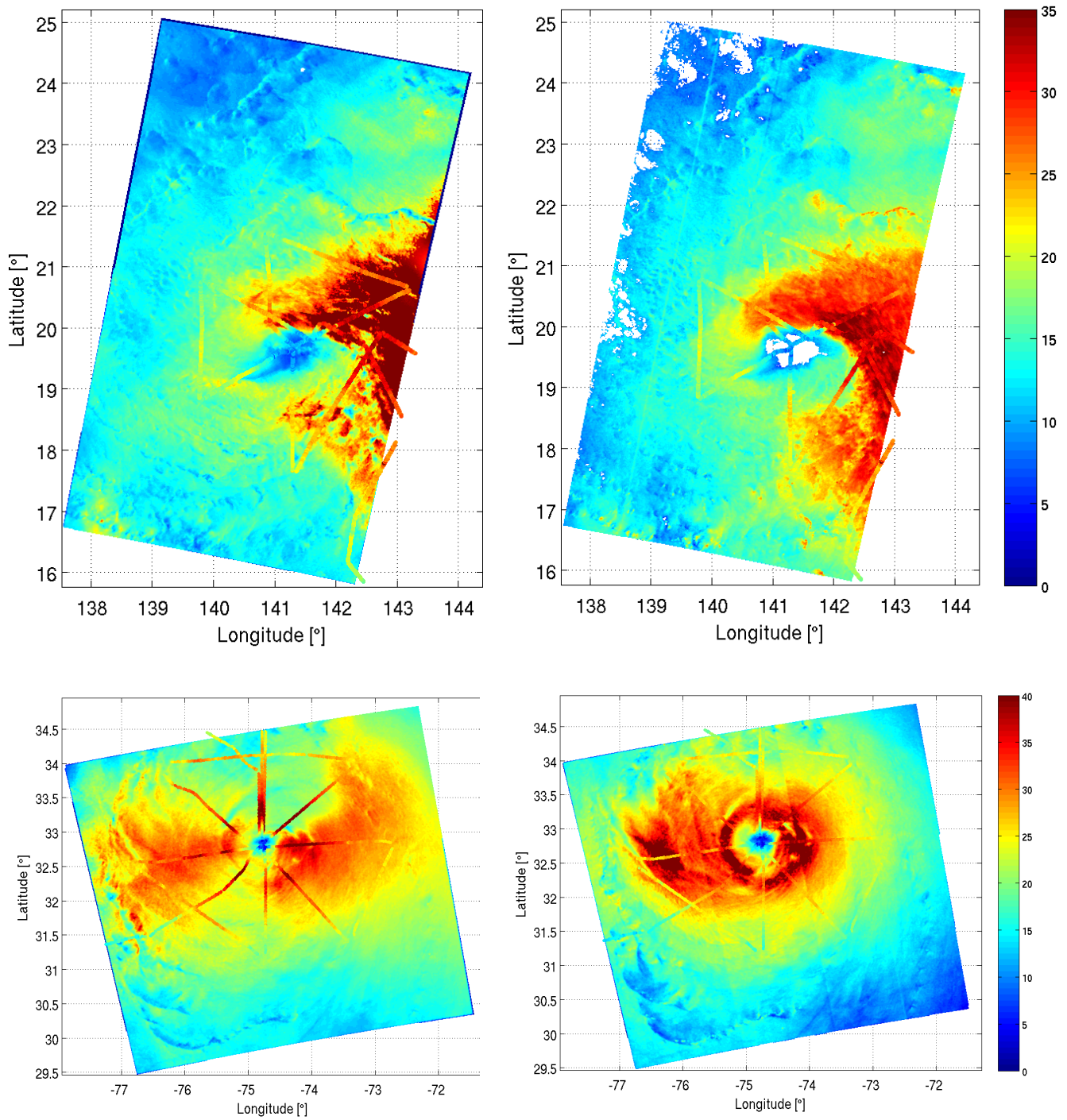


Figure 4: SAR retrieved wind fields of Tropical Storm Malakas acquired on 22 September 2010 at 20:29 UTC at HH pol (upper left) and at HV pol (upper right) as well as Hurricane Earl acquired on 2 September 2010 at 22:59 UTC at VV pol (lower left) and VH pol (lower right). For comparison the wind speed results from the SFMR flights are superimposed to the SAR retrieved winds. The color scales represent wind speeds in m/s.

Figure 4 (upper panel) depicts the SAR retrieved wind fields of Typhoon Malakas (at the time a tropical storm) with the superimposed wind speed measurements from SFMR. The left hand side shows wind fields retrieved from the HH pol data and the right hand side from the HV pol data respectively. The lower panel of Figure 4 shows the wind fields of Hurricane Earl (at the time of acquisition a category 2 storm) with the available SFMR wind speed measurements. In this case the data were acquired at VV pol (left hand side) and VH pol (right hand side). The comparison to SFMR data clearly show a much better agreement for the cross pol data in particular at the very high wind speeds. Also the typical ‘hour glass effect’ observed in co-pol data, meaning the under estimated wind speed measurements at up and down wind at high wind speeds, is not observed in cross pol retrieved wind fields. Furthermore, the GMF of cross pol data does not show saturation effects of the NRCS at high wind speeds. However, at low wind speeds (<10 m/s) cross pol data are strongly biased by the noise floor such that they cannot be used for wind speed retrieval.

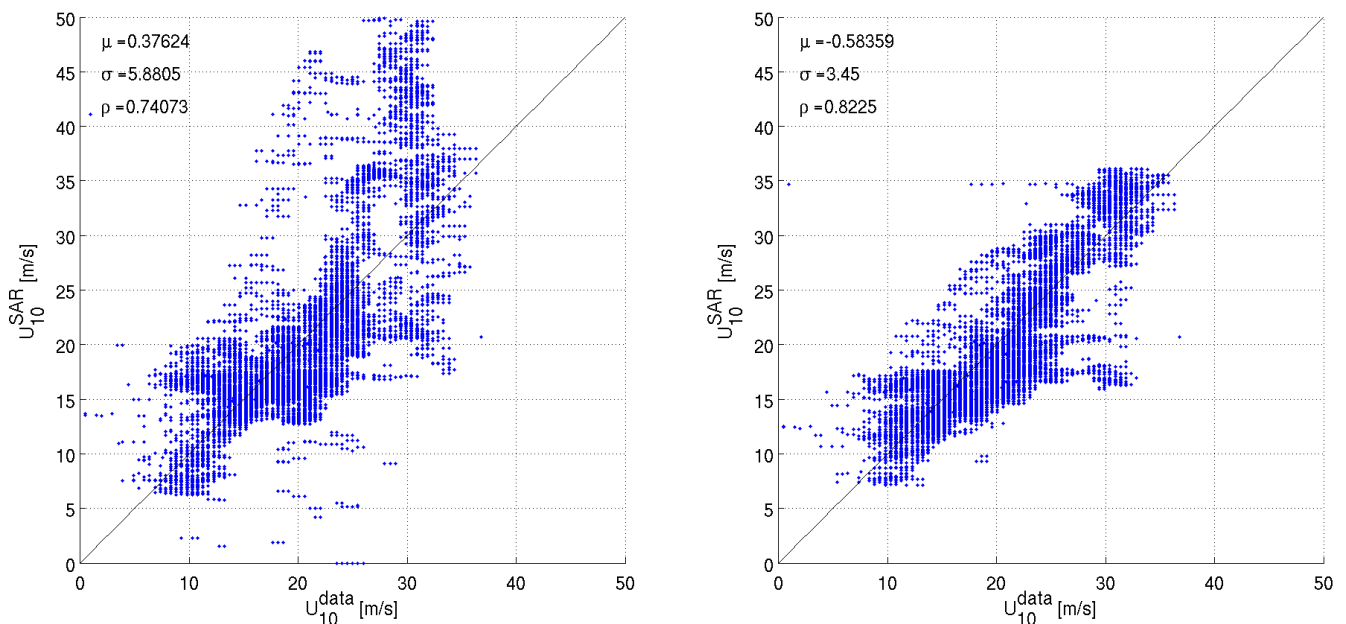


Figure 5: Scatter plots of comparison of SFMR wind speeds versus SAR retrieved wind speeds from co-pol data (left hand side) and cross pol data (right hand side). The main statistical parameters such as bias (μ), standard deviation (σ), and correlation (ρ) are given in the upper left of each scatter plot.

The overall comparison of all C-band SAR retrieved wind fields versus wind speeds collected from different sensors during the ITOP experiments are shown in the scatter plots of Figure 5. All SFMR measurements have been corrected for the movement of the storm as well as converted to 10 minute mean wind speeds at 10 meter height. The comparison of co-pol retrieved wind speeds resulted in a standard deviation of 5.9 m/s with a bias of 0.38 m/s, and in the case of cross pol data in a standard deviation of 3.5 m/s with a bias of -0.58 m/s. Further investigations of the wind speed error dependence showed that the error of co-pol retrieved winds increases significantly with wind speed and decreasing incidence angles. In case of cross pol data the increase in error with wind speed and incidence angle is significantly less obvious.

RESULTS

We have developed a correction scheme for SAR data that removes processing artifacts as well as noise contributions that significantly improved the quality of SAR data. We also have developed a GMF for cross pol data, which enables, in combination with co-pol data, to measure hurricane force wind fields with a good accuracy over the entire range of wind speeds. Using Radasat-2 C-band SAR data acquired in dual polarization mode (HH and HV) it enables to measure a tropical cyclone wind field with a resolution of approximately 1 km and an error in wind speed of approximately 3.6 m/s.

IMPACT/APPLICATIONS

The significantly improved accuracies of SAR retrieved winds of tropical cyclones using SAR data acquired at cross pol, provides a unique approach to get detailed information of tropical cyclones in near real time. This information will improve the understanding as well as prediction of tropical storms.

TRANSITIONS

The new algorithms are now being ingested into the SAR Typhoon Processing System at CSTARS, University of Miami, and will be tested in particular with respect to operational near real time processing.

REFERENCES

- Hersbach, H., Comparison of C-Band Scatterometer CMOD5.N Equivalent Neutral Winds with ECMWF. *J. Atmos. Oceanic Technol.*, **27**, 721–736, doi 0.1175/2009JTECHO698.1, 2010.
- Horstmann J., W. Koch, S. Lehner, and R. Tonboe, “Wind retrieval over the ocean using synthetic aperture radar with C-band HH polarization”, *IEEE Trans. Geosci. Remote Sens.*, vol. 38, no. 5, pp. 2 122–2 131, 2000.
- Horstmann J., W. Koch, S. Lehner, and R. Tonboe, “Ocean winds from RADARSAT-1 ScanSAR”, *Can. J. Remote Sens.*, Vol. 28(3), pp. 524-533, 2002.
- Horstmann, J., and W. Koch, “Comparison of SAR wind field retrieval algorithms to a numerical model utilizing ENVISAT ASAR data”, *IEEE Journal of Oceanic Engineering*, 30 (Iss.3), 508-515, doi 10.1109/JOE.2005.857514, 2005.
- Horstmann, J., “Estimating Winds from Synthetic Aperture Radar under Typhoon Conditions”, *ONR Annual Report*, 6 pp., 2011.
- Horstmann, J., S. Falchetti, S. Maresca, C. Wackerman, M. Caruso and H. Graber, “High resolution Tropical Cyclone Winds Retrieved from Satellite Borne C-band Cross Polarized Synthetic Aperture Radar”, *IEEE Trans. Geosci. Remote Sens.*, submitted 2012.
- Romeiser, R., J. Horstmann, M.J. Caruso, and H.C. Graber, “A Descalloping Post-Processor for ScanSAR Images of Ocean Scenes”, *IEEE Trans. Geosci. Remote Sens.*, in press 2012.
- Thompson, D.R., J. Horstmann, A. Mouche, N.S. Winstead, R. Sterner, and F.M. Monaldo, “Comparison of high-resolution wind fields extracted from TerraSAR-X SAR imagery with

predictions from the WRF mesoscale model”, *J. Geophys. Res.*, Vol. 17, C02035, 17 pp., DOI:10.10029/2011JC007526, 2012.

Touzi, R., P. W. Vachon, and J. Wolfe, “Requirement on antenna cross-polarization isolation for the operational use of C-band SAR constellations in maritime surveillance”, *IEEE Geosci. Remote Sens. Lett.*, 7, 861–865, 2010.

Wackerman, C.C., W.G. Pichel, and P. Clemente-Colon, ”A projection method for automatic estimation of wind vectors with RADARSAT SAR imagery”, *Proc. 2nd Workshop on Coastal and Marine Applications of SAR*, Svalbard, Norway, ESA SP-565, p. 55, 2003.

PUBLICATIONS

Horstmann, J., S. Falchetti, S. Maresca, C. Wackerman, M. Caruso and H. Graber, “High Resolution Tropical Cyclone Winds Retrieved from Satellite Borne C-band Cross Polarized Synthetic Aperture Radar”, *IEEE Trans. Geosci. Remote Sens.*, submitted 2012.

Romeiser, R., J. Horstmann, M.J. Caruso, and H.C. Graber, “A Descalloping Post-Processor for ScanSAR Images of Ocean Scenes”, *IEEE Trans. Geosci. Remote Sens.*, in press 2012.

Thompson, D.R., J. Horstmann, A. Mouche, N.S. Winstead, R. Sterner, and F.M. Monaldo, “Comparison of high-resolution wind fields extracted from TerraSAR-X SAR imagery with predictions from the WRF mesoscale model”, *J. Geophys. Res.*, Vol. 17, C02035, 17 pp., DOI:10.10029/2011JC007526, 2012.